J Sign Process Syst
DOI 10.1007/s11265-013-0833-4

Decision-Directed Channel Estimation Implementation for Spectral Efficiency Improvement in Mobile MIMO-OFDM

Johanna Ketonen · Markku Juntti · Jari Ylioinas · Joseph R. Cavallaro

Received: 20 June 2012 / Revised: 12 July 2013 / Accepted: 15 July 2013

Abstract Channel estimation algorithms and their implementations for mobile receivers are considered in this paper. The 3GPP long term evolution (LTE) based pilot structure is used as a benchmark in a multiple-input multiple-output (MIMO) orthogonal frequency division multiplexing (OFDM) receiver. The decision directed (DD) space-alternating generalized expectation-maximization (SAGE) algorithm is used to improve the performance from that of the pilot symbol based least-squares (LS) channel estimator. The performance is improved with high user velocities, where the pilot symbol density is not sufficient. Minimum mean square error (MMSE) filtering is also used in estimating the channel in between pilot symbols. The pilot overhead can be reduced to a third of the LTE pilot overhead with DD channel estimation, obtaining a ten percent increase in data throughput. Complexity reduction and latency issues are considered in the architecture design. The pilot based LS, MMSE and the SAGE channel estimators are implemented with a high level synthesis tool, synthesized with the UMC 0.18 μm CMOS technology and the performance-complexity trade-offs are studied. The MMSE estimator improves the performance from the simple LS estimator with LTE pilot structure and has low power consumption. The SAGE estimator has high power consumption but can be used with reduced pilot density to increase the data rate.

Keywords Channel estimation · MMSE · SAGE · EM · ASIC

This research has been supported in part by Tekes, the Finnish Funding Agency for Technology and Innovation, Nokia Siemens Networks, Renesas Mobile Europe, Elektrobit, Xilinx and Academy of Finland as well as the Nokia Foundation. The Rice University co-author was supported in part by the NSF under grants CNS-1265332, ECCS-1232274, and EECS-0925942.

J. Ketonen (✉) · M. Juntti
Department of Communications Engineering,
Centre for Wireless Communications, University of Oulu,
P.O. Box 4500, 90014 Oulu, Finland
e-mail: johannak@ee.oulu.fi

M. Juntti
e-mail: markku.juntti@ee.oulu.fi

J. Ylioinas
Nokia Siemens Networks,
P.O. Box 319, 90651 Oulu, Finland
e-mail: jari.ylioinas@nsn.com

J. R. Cavallaro
Rice University, 6100 Main Street,
Houston, TX 77005-1892, USA
e-mail: cavallar@rice.edu

1 Introduction

Multiple-input multiple-output (MIMO) systems offer an increase in capacity or diversity. Orthogonal frequency division multiplexing (OFDM) is a popular technique for wireless high data rate transmission because it enables efficient use of the available bandwidth and a simple implementation. The combination of MIMO and OFDM is a popular wireless access scheme and it has been adopted in the third generation partnership project (3GPP) long term evolution (LTE) and LTE advanced (LTE-A) standards [1] as well as in the Worldwide Interoperability for Microwave Access (WiMAX) system.

The reference signals or pilot symbols [2] used in channel estimation are placed in the OFDM time-frequency grid at certain intervals in the LTE system [1]. The interval may not be sufficiently short when the user velocity is high and the channel is fast fading. The high mobility scenario, which

Published online: 04 August 2013

is included in the LTE-A requirements, calls for the use of spatial multiplexing when the channel state information (CSI) at the transmitter becomes outdated for transmission adaptation. Furthermore, the pilot overhead increases with the number of MIMO streams. It becomes more problematic as the number of antennas in the system increases. Additionally, channel estimation based on only pilot symbols does not utilize the channel information available in the data decisions. Decision directed (DD) channel estimation can be used to improve the performance by exploiting the information on the non-pilot symbols or to reduce the pilot overhead by transmitting data symbols instead of pilot symbols.

The least-squares (LS) method attempts to minimize the squared difference between the received signal and the known pilot symbols or the data decisions [3]. Maximum likelihood (ML) channel estimation is equivalent to LS estimation with additive white Gaussian noise when the number of pilot symbols is larger than the channel length [4]. The recursive LS (RLS) algorithm can be used to enhance the channel estimation performance but it is most suitable for slow fading channels [5]. Using the LS channel estimation with data decisions would incur a high complexity in the receiver due to the large matrix inversion. The expectation-maximization (EM) algorithm [6] can be used to calculate the maximum likelihood (ML) estimate iteratively, avoiding the matrix inversion. The space-alternating generalized expectation-maximization (SAGE) algorithm [7, 8] provides faster convergence than the traditional EM algorithms. The SAGE algorithm has been considered for channel estimation jointly with detection and decoding in [9] and for MIMO-OFDM in [10]. Minimum mean square error (MMSE) filtering can be used in channel estimation to improve the performance by including the time domain (TD) and spatial correlation in the estimation [11, 12]. An implementation of an approximate linear MMSE channel estimator was presented in [13] and an implementation of a channel estimator for fading channels was discussed in [14] and [15]. The performance and the complexity in number of multiplications of the LS and SAGE algorithms were presented in [16] but the MMSE algorithm or implementations of the channel estimation algorithms were not included. Several algorithms for channel estimation in high velocity scenarios have been proposed. However, the actual implementation cost or a performance-complexity comparison of the algorithms has not been previously discussed. Thus, this is the scope of the paper.

In this paper, performance of the LS, MMSE and SAGE channel estimation algorithms is studied using the LTE pilot symbol structure [1] as a benchmark. Two throughput decreasing issues are addressed, namely the fast fading or high mobility scenario with insufficient pilot symbol density and the high pilot overheads from the MIMO pilot symbols. The SAGE channel estimator is used in the iterative receiver to improve the performance when the pilot symbol density is too low, i.e. in high velocity cases. MMSE filtering is also used in between pilot symbols to improve the channel estimates and the performance is compared to that of the SAGE estimator. The throughput can be increased by replacing some of the pilot symbols with data symbols and using the SAGE algorithm to compensate for the performance loss caused by the decreased pilot density. The theoretical complexity of the channel estimation algorithms is presented and some complexity-performance trade-off aspects of the SAGE algorithm are considered. The architecture and implementation results in gate counts and power consumption for the pilot symbol based LS, MMSE and the DD SAGE channel estimators are presented for the 2×2 and 4×4 antenna systems. For a more energy efficient solution, a longer latency for the channel estimator is considered. The impact of generating a timely channel estimate for the detector on the performance and complexity is then discussed.

The paper is organized as follows. The system model is presented in Section 2. The channel estimation algorithms are introduced in Section 3 and the performance examples are discussed in Section 4. Some complexity reducing techniques are considered in Section 5, the implementation results are presented in Section 6 and the conclusions are drawn in Section 7.

2 System Model

An OFDM based spatial multiplexing MIMO transmission system with N transmit (TX) and M receive (RX) antennas, where $N \leq M$, is considered in this paper. The LTE standard specifies a maximum of two separately encoded data streams [1]. Layered space-time architecture with horizontal encoding is applied, i.e. the two data streams are encoded and decoded separately. In the 4×4 antenna system, each of the two streams are multiplexed onto two antennas; the first stream is multiplexed onto the first and second antenna and the second stream onto the third and fourth antenna. The system model is shown in Fig. 1. The soft symbol estimates from the decoder are used in the channel estimation.

The received frequency domain (FD) signal vector $\underline{\mathbf{y}}(n)$ on the m_Rth receive antenna at discrete time index n after the discrete Fourier transform (DFT) can be described as

$$\underline{\mathbf{y}}_{m_R}(n) = \mathbf{X}(n)\underline{\mathbf{F}}\mathbf{h}_{m_R}(n) + \mathbf{w}_{m_R}(n), \tag{1}$$

where $\mathbf{X}(n) = [\mathbf{X}_1, ..., \mathbf{X}_N] \in \mathbb{C}^{P \times NP}$ is the transmitted signal over P subcarriers and N transmit antennas, $\mathbf{w}_{m_R} \in \mathbb{C}^P$ Gaussian noise, $\underline{\mathbf{F}} = \mathbf{I}_N \otimes \mathbf{F}$ is a $NP \times NL$ matrix from the DFT matrix with $[\mathbf{F}]_{u,s} = \frac{1}{\sqrt{P}} e^{-j2\pi us/P}, u = 0, ..., P-$

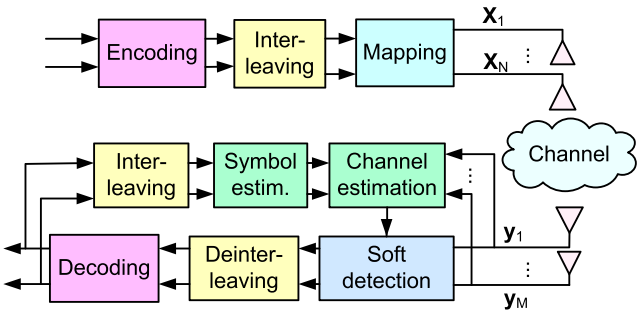

Figure 1 The MIMO-OFDM transceiver.

1, $s = 0, ..., L-1$, L is the length of the channel impulse response and $\mathbf{h}_{m_R} \in \mathbb{C}^{NL}$ is the time domain channel vector from the transmit antennas to the m_Rth receive antenna. The entries of the diagonal matrix $\mathbf{X}_{m_T} \in \mathbb{C}^{P\times P}$ are from a complex quadrature amplitude modulation (QAM) constellation Ω and $|\Omega| = 2^Q$, where Q is the number of bits per symbol and $m_T = 1, ..., N$ and $m_R = 1, ..., M$.

The cell-specific reference signal or pilot symbol positions in LTE resource elements are illustrated in Fig. 2, where the downlink slot consist of OFDM symbols i, where $i = 0, .., 6$ for the normal cyclic prefix [1]. Each element in the grid corresponds to a resource element. Reference signals are transmitted in the first, second and fifth OFDM symbols. The reference signals in the first antenna port are illustrated with black, in the second with vertical stripes, in the third with horizontal stripes and in the fourth port with diagonal stripes. Nothing is transmitted on the other antenna ports when a reference signal is transmitted on one antenna port. The reference signals for each antenna port are mapped to every 6th resource element in frequency. Quadrature phase shift keying (QPSK) modulated reference signals are assumed.

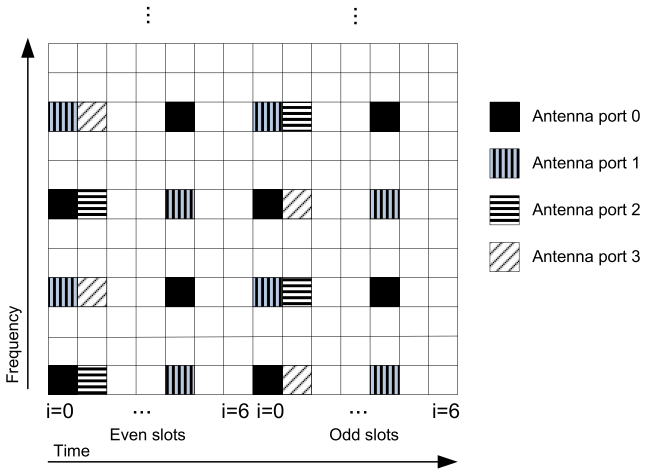

Figure 2 The LTE pilot structure.

The pilot overhead in the 2×2 MIMO is roughly 9.5 % and in the 4×4 MIMO 14 %. With 8×8 MIMO the pilot overhead could be more than 20 % when the demodulation reference signals are used. In LTE-A, user specific or demodulation reference signals are specified to support up to 8 transmit antennas [1]. With spatial multiplexing, demodulation reference signals can be transmitted for all antennas in the last two OFDM symbols in a slot. Reference signals for up to four antennas can be transmitted in the same subcarrier and orthogonal cover codes are used to achieve time and frequency domain orthogonality. The demodulation reference signals can be used with precoding so that the channel estimate obtained from the reference signals corresponds to the precoded channel. The demodulation reference signals are not considered in this paper.

3 Channel Estimation

The receiver structure is presented in Fig. 3. The LS channel estimator is used in calculating the channel estimates from pilot symbols. The received signal vector is transformed into frequency domain before the LS channel estimation. The LS channel estimate can be filtered with an MMSE filter. The channel impulse response result from the LS or MMSE estimator has to be transformed into frequency domain for the detector with the second fast Fourier transform (FFT). The DD SAGE channel estimator can be used in addition to the LS estimator. The pilot based LS estimator provides initial channel estimates for the SAGE. The soft symbols are calculated from the decoder outputs and are transformed into time domain for the SAGE channel estimator. The SAGE channel estimator also takes the time domain received signal as input.

3.1 LS Channel Estimation

The LS estimate of the channel can be calculated as

$$\hat{\mathbf{h}}^{\mathrm{LS}}_{m_R}(n) = \left(\mathbf{F}^{\mathrm{H}}\mathbf{X}^{\mathrm{H}}(n)\mathbf{X}(n)\mathbf{F}\right)^{-1}\mathbf{F}^{\mathrm{H}}\mathbf{X}^{\mathrm{H}}(n)\underline{\mathbf{y}}_{m_R}(n), \qquad (2)$$

where $\mathbf{X}$ contains the pilot symbols or if used in a DD mode, the symbol decisions. The calculation of the LS channel estimate from the pilot symbols is simple as the matrix

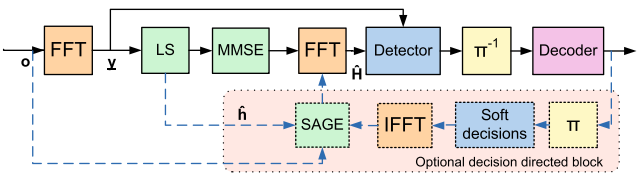

Figure 3 The receiver structure.

inversion can be calculated in advance and the only calculation to be performed in real time is multiplication with the received signal. When using the LS estimator in a DD mode, the $NL \times NL$ matrix inversion induces a high computational complexity.

3.2 MMSE Channel Estimation

In order to exploit the time domain correlation of the channel and to take into account the impact of the noise, the LS channel estimate can be filtered with an MMSE filter [3]

$$\hat{\mathbf{h}}^{\mathrm{MMSE}}_{m_R,m_T,l}(n) = \mathbf{W}^{\mathrm{H}}_{m_R,m_T,l}(n)\hat{\mathbf{h}}^{\mathrm{LS}}_{m_R,m_T,l}, \tag{3}$$

where the LS channel estimate vector for the lth tap from the m_Tth transmit antenna to the m_Rth receive antenna

$$\hat{\mathbf{h}}^{\mathrm{LS}}_{m_R,m_T,l} = \left[\hat{h}^{\mathrm{LS}}_{m_R,m_T,l}(n_1)...\hat{h}^{\mathrm{LS}}_{m_R,m_T,l}(n_{N_P})\right]^{\mathrm{T}} \in \mathbb{C}^{N_P \times 1} \tag{4}$$

contains the LS channel estimates from the duration of the filtering window. N_P is the number of OFDM symbols with pilot symbols in a filtering window and $m_T = 1, ..., N$ and $m_R = 1, ..., M$ are the transmit and receive antenna indices. The filtering vector $\mathbf{W}_{m_R,m_T,l}(n)$ is defined as

$$\mathbf{W}_{m_R,m_T,l}(n) = \mathbf{\Sigma}^{-1}_{\hat{\mathbf{h}}^{\mathrm{LS}}_{m_R,m_T,l}} \mathbf{\Sigma}^{\mathrm{H}}_{m_R,m_T,l}, \tag{5}$$

where the cross-covariance matrix between $h_{m_R,m_T,l(n)}$ and $\hat{\mathbf{h}}^{\mathrm{LS}}_{m_R,m_T,l}$ is

$$\mathbf{\Sigma}_{m_R,m_T,l} = [\rho(n-n_1)...\rho(n-n_{N_P})]\Sigma_{\mathbf{h}_l} \tag{6}$$

and the auto-covariance matrix is

$$\mathbf{\Sigma}_{\hat{\mathbf{h}}^{\mathrm{LS}}_{m_R,m_T,l}} = \begin{bmatrix} \rho(n_1-n_1) & \cdots & \rho(n_1-n_{N_P}) \\ \vdots & \ddots & \vdots \\ \rho(n_{N_P}-n_1) & \cdots & \rho(n_{N_P}-n_{N_P}) \end{bmatrix} \Sigma_{\mathbf{h}_{m_R,m_T,l}} + \mathbf{\Sigma}_w. \tag{7}$$

The noise covariance matrix $\mathbf{\Sigma}_w = \sigma^2\mathbf{I} \in \mathbb{R}^{(N_p \times N_p)}$, $\Sigma_{\mathbf{h}_{m_R,m_T,l}} = E\left(h^*_{m_R,m_T,l}h_{m_R,m_T,l}\right)$ and $\rho(n-n')$ is the temporal correlation between the channel taps at times n and n' [12]. In order to avoid the calculation of the spatial correlation $\Sigma_{\mathbf{h}_l}$, it can be left out from Eqs. 6 and 7. This only has a minor impact on the performance as presented in Section 4. It also enables the use of precalculated MMSE filter coefficients, where the predetermined values for σ^2 and user velocity are used. The coefficients can be calculated for a set of σ^2 and velocity values and the coefficients closest to the estimated values can be used. Since $\rho(n-n) = 1$ and $\mathbf{\Sigma}_w$ contains σ^2 on its diagonal, the precalculated coefficients can be obtained by substituting the known values in Eq. 5. The MMSE filter coefficients can be then precalculated as

$$\begin{bmatrix} 1+\sigma^2 & \cdots & \rho(n_1-n_{N_P}) \\ \vdots & \ddots & \vdots \\ \rho(n_{N_P}-n_1) & \cdots & 1+\sigma^2 \end{bmatrix}^{-1} \begin{bmatrix} \rho(n-n_1) \\ \vdots \\ \rho(n-n_{N_P}) \end{bmatrix}, \tag{8}$$

where the temporal correlation is distributed according to Jake's model and can be written as

$$\rho(n-n') = J_0(2\pi f_d(n-n')T_B) \tag{9}$$

and J_0 denotes the zeroth-order Bessel function of the first kind, f_d is the Doppler frequency and T_B is the OFDM symbol duration.

3.3 SAGE Channel Estimation

The EM algorithms consist of an expectation and a maximization step. The "complete" data is estimated in the expectation step and the channel estimate is updated in the maximization step. The frequency domain SAGE algorithm provides an iterative solution of the decision directed LS estimate in Eq. 2. The time domain SAGE algorithm [17] can be used instead of the FD SAGE channel estimator to avoid the matrix inversion required with non-constant envelope modulations. The time domain received signal $\mathbf{o}$ is viewed as the "incomplete" data and $\mathbf{z}$ as the "complete" data, which is iteratively updated along with the channel estimate $\hat{h}_{m_T,m_R,l}(n)$. The time domain symbol estimates from the decoder are denoted as $\bar{\mathbf{x}}$. The time domain SAGE algorithm calculates the channel estimates with iterations

$$\hat{\underline{\mathbf{z}}}^{(i)}_{m_T,m_R,l} = \hat{\underline{\mathbf{z}}}^{(i)}_{m_T,m_R,l} + \left[\mathbf{o}_{m_R} - \sum_{m'_T=1}^{M_T}\sum_{l'=0}^{L-1}\hat{\underline{\mathbf{z}}}^{(i)}_{m'_T,m_R,l'}\right] \tag{10}$$

$$\hat{h}^{(i+1)}_{m_T,m_R,l}(n) = \frac{\bar{\mathbf{x}}^{\mathrm{H}}_{m_T,l}\hat{\underline{\mathbf{z}}}^{(i)}_{m_T,m_R}(n)}{\bar{\mathbf{x}}^{\mathrm{H}}_{m_T,l}\bar{\mathbf{x}}_{m_T,l}} \tag{11}$$

$$\hat{\underline{\mathbf{z}}}^{(i+1)}_{m_T,m_R,l}(n) = \bar{\mathbf{x}}_{m_T,l}\hat{h}^{(i+1)}_{m_T,m_R,l} \tag{12}$$

$$\hat{\underline{\mathbf{z}}}^{(i+1)}_{m''_T,m_R,l''}(n) = \hat{\underline{\mathbf{z}}}^{(i)}_{m''_T,m_R,l''} \tag{13}$$

The channel estimator is initialized with the channel estimate $\hat{h}^{(0)}_{m_T,m_R,l}$ from the previous OFDM symbol as

$$\hat{\underline{\mathbf{z}}}^{(0)}_{m_T,m_R,l}(n) = \bar{\mathbf{x}}_{m_T,l}\hat{h}^{(0)}_{m_T,m_R,l}. \tag{14}$$

4 Performance Comparison

The simulation parameters are presented in Table 1 and the vehicular channel model parameters [18] in Table 2. The

Table 1 Simulation parameters.

Coding	Turbo coding with 1/2 code rate
Carrier frequency	2.4 GHz
Modulation scheme	16-QAM
Number of subcarriers	512 (300 used), 5 MHz bandwidth
Symbol duration	71.4 μs

simulator for the MIMO fading channel model was introduced in [19] and it includes temporal, spatial and spectral correlation. The detector used in the simulations is a K-best list sphere detector (LSD) [20] with list size 8 in the 2×2 antenna system and 16 in the 4×4 antenna system. Turbo coding was performed over one OFDM symbol. The user velocities of 50 km/h and 100 km/h were assumed where the corresponding Doppler frequencies were 111 Hz and 222 Hz.

Mitigation of inter-carrier interference (ICI) caused by very high mobile velocities is out of the scope of this work. The remaining frequency offset after frequency synchronization may be modeled with increased noise at the receiver [21]. Furthermore, the algorithms considered in this paper are not among the most suitable algorithms for very high velocities where the ICI would be the most dominant.

The throughput can be increased by using half of the LTE reference signals along with the decision directed channel estimation. The pilot symbols are then transmitted only in the first OFDM symbol in a slot and data is transmitted instead of pilot symbols in the other OFDM symbols which is denoted in the figures as 1 pilot. In this scenario, the pilot symbols are transmitted in the same subcarriers in the first OFDM symbol as in the LTE scheme. Channel estimation can be performed over several slots but this decreases the performance in high velocity scenarios.

In the following simulation results, LS channel estimation is used on the OFDM symbols with pilot symbols and the SAGE algorithm is used on the OFDM symbols without reference signals. The performance of the SAGE algorithm with transmitted data as the feedback, i.e. genie aided SAGE, is also shown in the figures. With the genie aided mode, pilots are transmitted in one OFDM symbol per slot where the LS estimator is used in estimating the channel. The MMSE channel estimator is precalculated with the

Table 2 Channel model parameters.

Number of paths	6
Path delays	[0, 310, 710, 1090, 1730, 2510] ns
Path powers	$-$[0, 1, 9, 10, 15, 20] dB
BS/MS antenna spacing	4 λ/ $\lambda/2$
BS average angle of departure	50°
MS average angle of arrival	67.5°
BS/MS azimuth spread	2 or 5°/ 35°

velocity of 70 km/h and the SNR of 26.5 dB in the 4×4 antenna system and 16.5 dB in the 2×2 antenna case as they were found to be suitable for most of the simulation cases. MMSE filtering is performed over one slot with the LTE pilot structure and over two slots with pilots in only one OFDM symbol as the MMSE filter needs at least two channel estimates to perform well. The filtering window is shifted when a new channel estimate is available from the LS estimator in order to obtain the most current estimates. This also decreases the latency from the case where channel estimation is performed on the whole slot before detection. Increasing the size of the filtering window with LTE pilot structure does not improve the performance.

The performance of the channel estimation algorithms is presented in Fig. 4 with a 4×4 antenna system. The communication system performance is usually characterized by frame error rate (FER). The transmission throughput is defined to be equal to the nominal information transmission rate of information bits times (1$-$FER). With pilot symbols in one OFDM symbol in a slot, denoted as 1 pilot, pilot symbols for all antennas are transmitted in the 1st OFDM symbol. The MMSE and SAGE estimators are able to compensate for the performance loss from the decreased pilot symbol density, unlike the LS estimator. The performance of the MMSE estimator is almost as good as with the SAGE estimator with the LTE pilot structure but when the pilot density is decreased, the performance difference is larger. The more dense LTE pilot structure can also have a positive impact on the performance in the lower SNRs where the quality of the received signal is worse.

The mean square error (MSE) results with a 100 km/h user velocity are shown in Fig. 5 where results of the MMSE filter with the known velocity, SNR and spatial correlation are also presented. The difference in performance of the MMSE filter with the known parameters is small to that

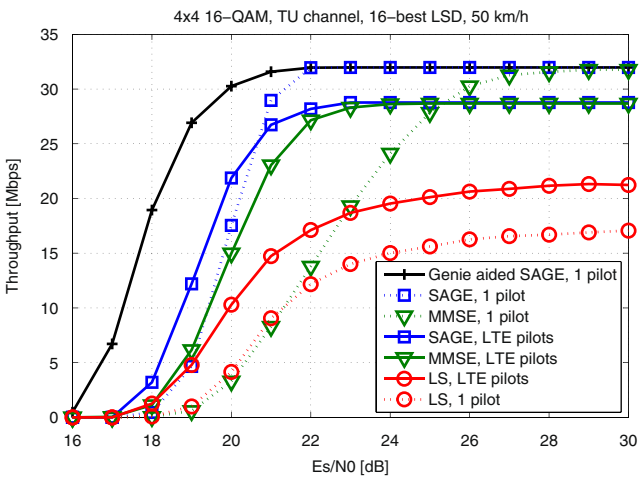

Figure 4 4×4 16-QAM data transmission throughput vs. SNR with different pilot densities and 50 km/h user velocity.

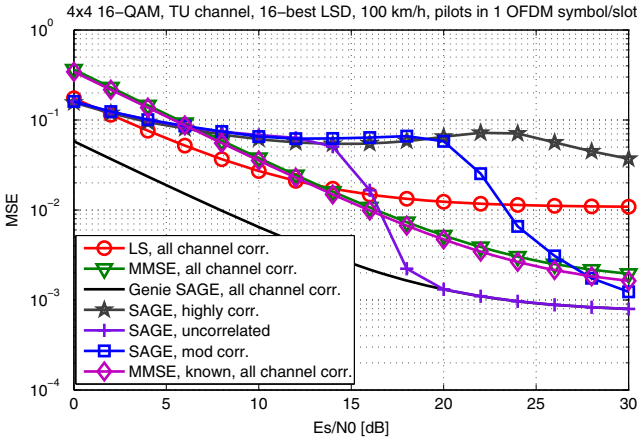

Figure 5 4×4 16-QAM MSE vs. SNR with different channels and 100 km/h user velocity.

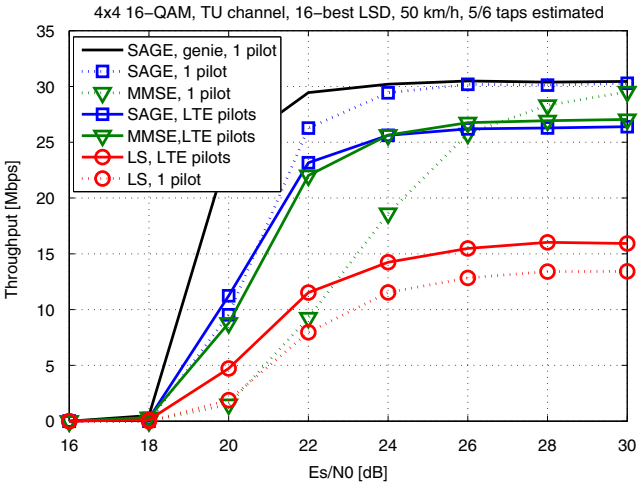

Figure 6 4×4 16-QAM data transmission throughput vs. SNR with estimated channel tap delays and 50 km/h user velocity.

of the MMSE filter with fixed parameters. Channel models with different amounts of correlation were used. The highly correlated channel is generated with the BS azimuth spread of 2 degrees and the moderately correlated channel with an azimuth spread of 5 degrees. The average channel condition number is 90 for the correlated channel, 30 for the moderately correlated channel and 10 for the uncorrelated channel. The condition number can be calculated as the ratio of the maximum and minimum singular value σ_1/σ_N, where the singular values are obtained from the diagonal matrix $\mathbf{\Sigma}$ with the singular value decomposition of the channel matrix $\mathbf{H} = \mathbf{U}\mathbf{\Sigma}\mathbf{V}^{\mathrm{H}}$. The performance is poor in the correlated channel. This is mostly due to the fact that the detector does not perform well in the highly correlated channel. This also has an impact on the performance of the SAGE algorithm as the quality of feedback from the detector is not high. The benefit obtained with the SAGE algorithm increases in the moderately correlated and uncorrelated channels.

The LTE pilot symbols for four transmit antennas were transmitted in different OFDM symbols in the slot. Transmitting pilot symbols for all four antennas in the same OFDM symbol in a slot improves the SAGE performance especially with high user velocities because there is no need to combine the channel estimate of the two antennas in the current OFDM symbol with the channel estimate of the other two antennas from the previous OFDM symbol. The SAGE estimator also gets a better initial guess of the channel when all pilot symbols are transmitted in the same slot and is able to estimate the channel well in the decision directed mode. With the LTE pilots, the MMSE filter performs well. However, the performance of the MMSE estimator degrades when the pilot symbol density decreases, i.e. the MMSE estimator needs a sufficient pilot symbol density to perform well. The MMSE estimator cannot be used effectively to improve the throughput by transmitting fewer pilots unlike the SAGE channel estimator.

The channel length and the delays of the taps were assumed to be known in the previous simulation results. However, in practice they would have to be estimated. Figure 6 shows the performance with estimated channel tap delays where only five taps were estimated when the number of channel taps was six. The tap delays were estimated by calculating a LS estimate $\hat{\mathbf{h}}$ for 20 taps and using the diagonal values $\mathbf{P}_{\mathrm{LS}} = \mathrm{diag}\left(\hat{\mathbf{h}}^{\mathrm{H}}\hat{\mathbf{h}}\right)$ to determine the strongest paths. Five paths from the estimated paths were used in channel estimation in Fig. 6. The genie aided SAGE estimator also uses only five channel taps. The performance degrades with the estimated taps compared to the known tap delays in Fig. 4 but the performance difference between the channel estimation algorithms does not change.

5 Complexity Reduction in Channel Estimation

The complexity of an algorithm can be measured, to some extent, by the number multiplications and additions performed during a certain processing time. The complexity of the time domain SAGE algorithm in number of multiplications is $N_c(8LNMS_i + 4N)$ and in the number of additions $N_c((2NL + 7)LNMS_i + 2N)$, where N_c is the number of subcarriers, L is the length of the channel and S_i is the number of SAGE iterations; $2N$ divisions are also needed. The number of multiplications in the LS channel estimator is $4N_rLN$, where N_r is the number of pilot symbols. The number of multiplications in the decision directed LS would be more than 12 million in a corresponding system when performing the $NL \times NL$ matrix inversion, where $N = 2$, $L = 6$ and $N_c = 512$ [17]. This is more than 60 times higher than in the DD SAGE estimator. The number of multiplications for obtaining the MMSE channel estimates with

precalculated coefficients is $2NMLN_PB$, where B is the length of the filtering window and N_p is the number of LS channel estimates used in the MMSE filtering.

5.1 SAGE Feedback Reduction

The feedback to the SAGE channel estimator, i.e. the number of data symbols calculated from the decoder outputs can be reduced. This lowers the complexity of the SAGE estimator but can cause some performance degradation. Figure 7 shows the performance with different numbers of feedback data symbols used in the SAGE channel estimation. SAGE with three iterations is equivalent to the SAGE with 1 pilot curve in Fig. 4. The number of multiplications and the performance degradation with different numbers of iterations S_i, channel taps L and feedback symbols used is presented in Table 3 in a system with 512 subcarriers. With half of the feedback symbols, every other subcarrier is used in the channel estimation. This decreases the complexity of the channel estimation almost by half. The performance can be increased with a higher number of SAGE iterations. In the 2×2 antenna case, a 0.5 dB performance degradation is observed when using every 4th symbol and 2 SAGE iterations. With 3 SAGE iterations, there is no performance degradation compared to using all the symbols. The estimation of the first 5 channel taps only will decrease the complexity but the performance will also degrade. A good performance with lower complexity can be achieved by estimating 6 taps with 1/4 of symbols and 4 SAGE iterations.

As a comparison, there are 4800 multiplications in the pilot symbol based LS channel estimator in the 2×2 system and 9600 in the 4×4 system. The number of multiplications in the list sphere detector used in simulations are 142 k in the 2×2 system and 984 k in the 4×4 system

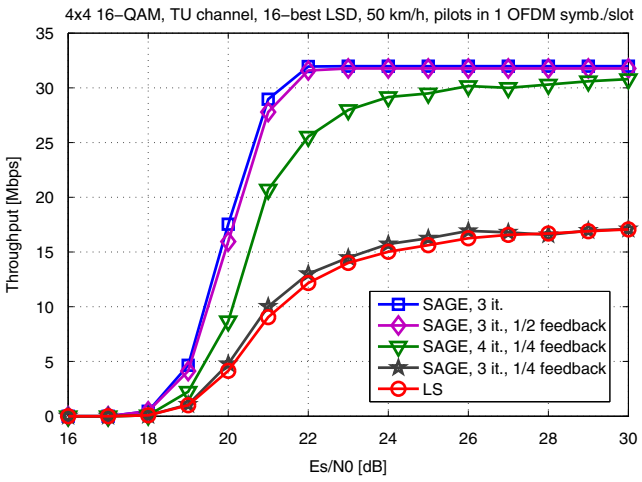

Figure 7 4×4 16-QAM data transmission throughput vs. SNR with different numbers of used symbols and 50 km/h user velocity.

Table 3 Number of multiplications with different numbers of iterations and symbols.

Symbols	S_i	L	Perf. degradation	Mult.
			2×2	
512	2	6	–	200704
256	2	6	±0 dB	100352
128	3	6	±0 dB	74752
128	2	6	−0.5 dB	50176
			4×4	
512	2	6	–	794624
256	3	6	±0 dB	593920
256	2	6	$-[2-4]$ dB	397312
256	3	5	$-[1-2]$ dB	495616
128	3	6	$-[3-5]$ dB	296960
128	4	6	−0.5 dB	395264

[22]. The complexity in terms of multipliers is almost half of that of a sphere detector but the achievable performance improvement can be significant.

5.2 Latency-Performance Trade-off

The LS channel estimation from the pilot symbols can be performed before detection in order to have a timelier channel estimate. However, the latency requirement of the channel estimator is less strict if channel estimation can be performed during detection. This can also have a major impact on the complexity. The alternative latencies in the receiver are presented in Fig. 8. In the top part of the figure, the channel estimators have a latency of one OFDM symbol, i.e. there is a delay in the channel estimates. Pilot symbols are received in the first OFDM symbol. The LS estimator then calculates the channel estimate during the detection of all data symbols in the first OFDM symbol. The LS channel estimate is used in the detection of the second OFDM symbol and as an input to the MMSE estimator or the SAGE estimator. The SAGE channel estimation can be performed when the decoding of the code word has finished. The data decisions of the first OFDM symbol are used to calculate the SAGE channel estimate while detecting the second OFDM symbol. The channel estimate is then used in the detection of the third symbol. Thus, the channel estimate used in the estimation is an estimate of the channel experienced two OFDM symbols ago. The other alternative is to use the result from the decision directed channel estimation in the detection of the next symbol as shown in the bottom part of the figure. The channel estimate used in detection corresponds to the channel experienced in the previous OFDM symbol. The MMSE estimator can be used to predict a more current channel estimate from the delayed LS estimates as

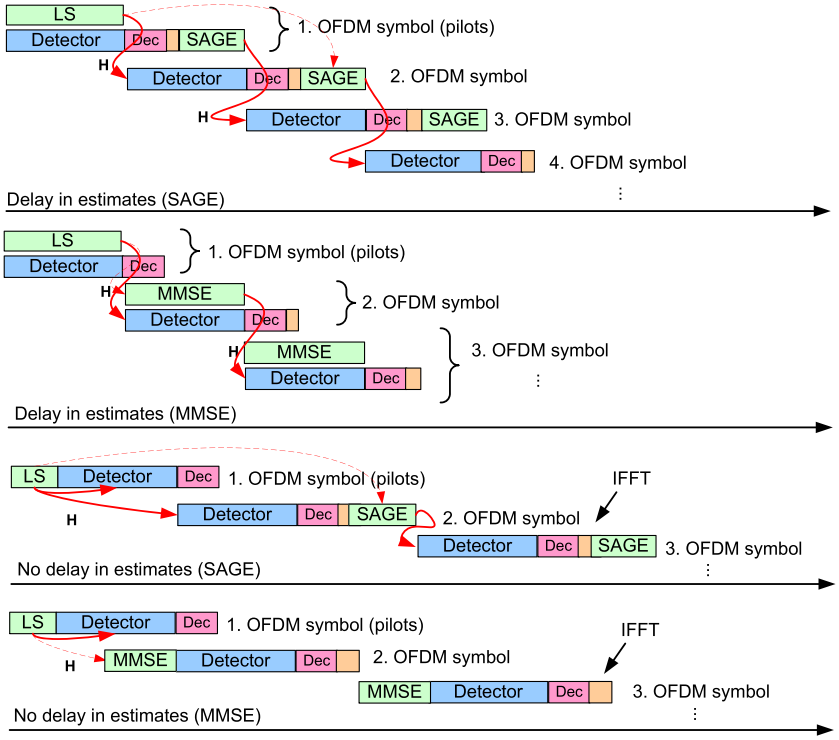

Figure 8 Receiver latency alternatives; delay/no delay in channel estimation.

the coefficients can be adjusted according to the delay of the LS estimate.

The performance of the channel estimators with different delays are presented in Fig. 9 with a 50 km/h user velocity. The results with delay in channel estimation are obtained with the scheduling from the top part of Fig. 8 and the results with no delay from the bottom part. The LS estimator was used with the LTE pilot structure and the SAGE estimator with a decreased pilot density, i.e. pilot symbols are transmitted in one OFDM symbol per slot. The impact of the delay on the performance increases with the user velocity. With 100 km/h user velocity, the performance degradation is more significant with the delayed channel estimation. The impact is high especially on the SAGE estimator which is sensitive to the initial guess, i.e. the channel estimate from the previous OFDM symbol.

6 Implementation of LS, MMSE and SAGE Channel Estimation

High level synthesis (HLS) is used to obtain the implementation results in this paper. Even though HLS tools have been developed for decades, only the tools developed in the last decade have gained a more widespread interest. The main reasons for this are the use of an input language, such as C, familiar to most designers, the good quality of results and their focus on digital signal processing (DSP) [23]. HLS tools are especially interesting in the context of rapid prototyping where they can be used for architecture exploration and to produce designs with different parameters.

The design process starts with a high level description of the functionality of the block. In this work, C code is used as the input language to the HLS tool. The high level description may have to be modified before being suitable for the HLS tool. In general, HLS tools first compile the input description, after which they allocate hardware resources and schedule the design before generating the register transfer level (RTL) implementation. Without any timing and

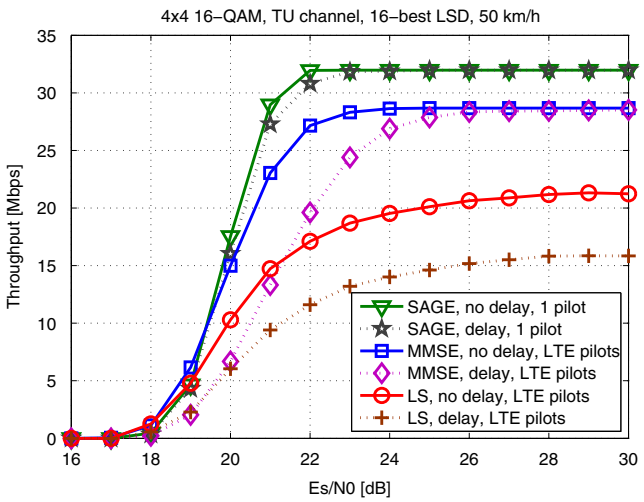

Figure 9 4×4 16-QAM data transmission throughput vs. SNR with different delays and 50 km/h user velocity.

allocation constraints in the input file, the generation of different architectures by changing the parameters in the tool is possible.

Catapult ® C Synthesis tool [24] was used in the implementation of the receivers. It synthesizes algorithms written in ANSI C++ and SystemC into hardware. This single source methodology allows designers to pick the best architecture for a given performance/area/power specification while minimizing design errors and reducing the overall verification burden. While the results may not always be as optimal as with hand-coded HDL, the tool allows experimenting with different architectures in a short amount of time and the comparison of different algorithms can be made, provided they are implemented with the same tool. The Synopsys Design Compiler was used in synthesizing the VHDL along with the UMC 0.18 μm CMOS technology. The FFTs are not included in the complexity estimations. The complexity and power consumption of each channel estimator is comparable only to other channel estimators presented in this paper as the results depend on the used implementation method and library. However, a few other channel estimation implementations from the literature will be briefly discussed.

6.1 Architecture and Memory Requirements

The pilot symbol based LS channel estimator includes complex multiplications of the LS coefficients $\mathbf{G}$ and the received data symbols. The calculation of each LNM channel coefficient includes P/N complex multiplications after which the results are added together. For a 2×2 antenna system, there are 80 channel coefficients to be calculated. The operations and their scheduling in the LS estimator in the 4×4 antenna system are shown in Fig. 10. The HLS tool performed the scheduling and resource allocation based on the constraints. The multiply and accumulate (MAC) operations for the real and complex part of the channel coefficient were scheduled in three clock cycles. The two multipliers from the first cycle can then be reused in the second cycle. As the LTE pilots are transmitted for two streams in one OFDM symbol, only half of the channel coefficients can be calculated. The 50 MAC operations were scheduled to be performed in 150 cycles with a 102 MHz clock frequency when a 71 μs delay was allowed for channel estimation. This leads to the three cycle schedule in Fig. 10.

The MMSE channel estimator consists of multiplications of the LS channel estimates with real valued coefficients. Each MMSE channel estimate coefficient $\hat{\mathbf{h}}^{\mathrm{MMSE}}_{m_R,m_T,l}$ is a composite of the N_P LS estimates from the filtering period. With the 4×4 system, $N_P = 3$ and the filtering period is 7 OFDM symbols. The MMSE channel estimator then performs 6 multiplications and 4 additions for each complex valued channel coefficient. The operations and the schedule of the MMSE estimator are presented in Fig. 11. One multiplier can be reused for all the multiply operations.

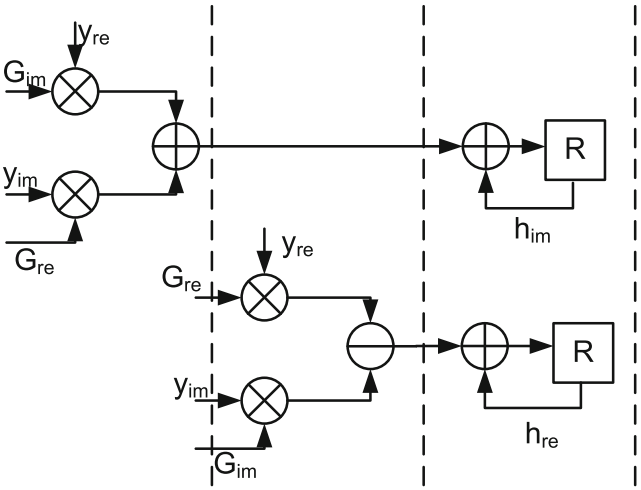

Figure 10 The operations and schedule of the LS channel estimator.

The architecture of the SAGE channel estimator for a 2×2 antenna system is presented in Fig. 12. Each block corresponds to Eqs. 10–14. The elements of $\bar{\mathbf{x}}_{m_T}$ in each stream are squared and the results are added together in the symbol multiplication part. The inverses of the results are multiplied with $\bar{\mathbf{x}}_{m_T}$. These calculations from Eq. 11 can be performed separately from the iterative channel tap calculations. For each channel tap, N_c iterations are performed. The channel tap iterations are initialized by multiplying the symbol decisions $\bar{\mathbf{x}}_{m_T}$ with the channel taps from the previous OFDM symbol in the block corresponding to Eq. 12. In later iterations, the channel taps from previous iterations are used. L multiplication results from N layers corresponding to the channel to each receive antenna are added together and subtracted from the received symbol from each receive antenna. The result is then added to the first $\bar{\mathbf{x}}_{m_T}\hat{h}_{m_T m_R}$ multiplication result in the block corresponding to Eq. 10 and multiplied with $\mathbf{x}_i^{-1}$ in the block corresponding to Eq. 11.

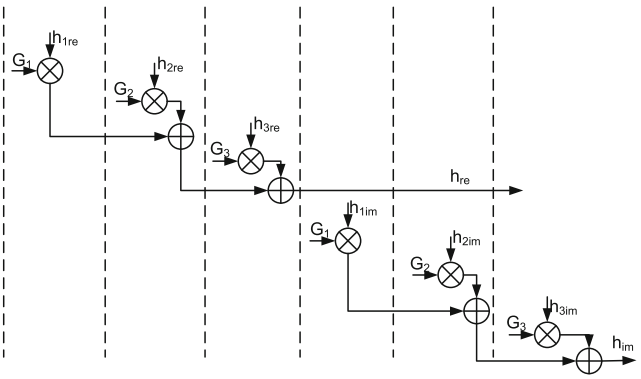

Figure 11 The operations and schedule of the MMSE channel estimator.

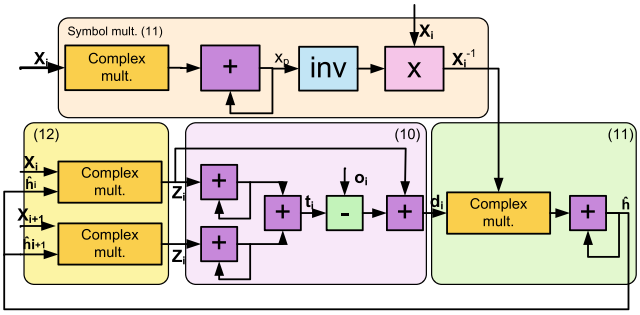

Figure 12 The architecture of the SAGE channel estimator.

A channel tap is obtained by adding together the results from the N_c iterations. The total number of iterations in calculating all the channel taps is $MNLS_iN_c$.

The precision of the variables required to sustain the performance close to that of the floating point variables were determined. The minimum word lengths for the channel estimators are presented in Table 4 in (word length, integer length, sign) format. The word lengths were determined with computer simulations using the same parameters as those in Section 4. The performance of the fixed point channel estimators compared to those of the floating point estimators are presented in Fig. 13. Some performance degradation is allowed in the fixed point estimators in order to keep the complexity low as reaching the floating point performance may require a considerable increase in the word lengths.

The total number of bits required in the variables, the bits out of the word length used for the integer part and if the variable is signed or unsigned are shown in the table. The variables in the SAGE channel estimator correspond to those in Fig. 12 and the corresponding block is denoted by Eqs. 10–12. The LS coefficients are the precalculated results of $\left(\mathbf{F}^{\mathrm{H}}\mathbf{X}^{\mathrm{H}}(n)\mathbf{X}(n)\mathbf{F}\right)^{-1}\mathbf{F}^{\mathrm{H}}\mathbf{X}^{\mathrm{H}}(n)$ from pilot symbols. The received signal vector $\bar{\mathbf{y}}$ is in frequency domain in the LS

Table 4 Word lengths in channel estimation.

SAGE		LS/MMSE	
Variable	(W, I, S)	Variable	(W, I, S)
$\bar{\mathbf{X}}_i$ (11)	(8,3,1)	$\underline{\mathbf{y}}$ (FD)	(16,4,1)
$\bar{\mathbf{X}}_i^{-1}$ (11)	(12,2,1)	LS coeff.	(12,2,1)
x_p (11)	(17,13,0)	$\hat{\mathbf{h}}_{\mathrm{LS}}$	(13,2,1)
$1/x_p$ (11)	(17,1,0)		
$\hat{\mathbf{h}}_i$ (11),(12)	(18,4,1)	MMSE coeff.	(13,2,1)
$\mathbf{t}_i$ (10)	(12,5,1)	$\hat{\mathbf{h}}_{\mathrm{MMSE}}$	(14,2,1)
$\hat{\mathbf{z}}_i$ (12)	(12,4,1)		
$\mathbf{o}_i$ (TD) (10)	(8,4,1)		
$\mathbf{d}_i$ (10)	(12,4,1)		

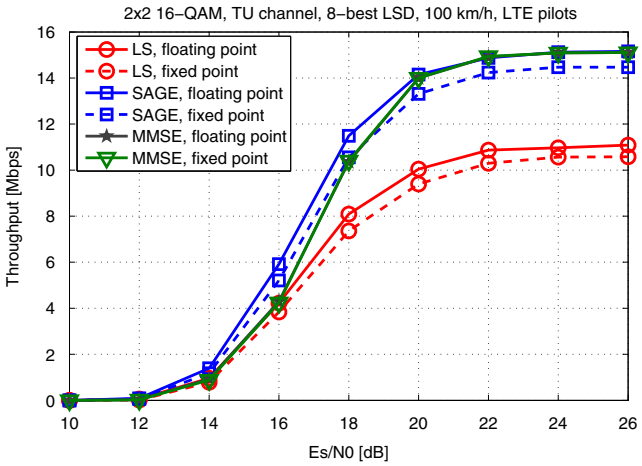

Figure 13 2×2 16-QAM data transmission throughput vs. SNR with fixed word lengths.

estimator and $\mathbf{y}_i$ is in time domain in the SAGE channel estimator. The MMSE coefficients are precalculated and real valued.

The amount of memory required to store the LS coefficients precalculated from the pilot symbols is 14.4 kbit assuming that the pilot symbols are the same in each OFDM symbol. The highest amount of memory in the MMSE filter is needed in storing the LS channel estimates from N_P OFDM symbols. The required amount of memory is 17.5 kbit in the 4×4 antenna system. In the SAGE channel estimator, the memory requirement for the symbol expectations $\bar{\mathbf{x}}_i$ is 16.4 kbit in the 2×2 antenna system and 32.8 kbit in the 4×4 antenna system. The highest amount of memory in the SAGE estimator would be the 1.2 Mbit for storing the interim results for $\hat{\mathbf{z}}_i$ but this is partly included in the following implementation results unlike the previously discussed memory requirements for the LS and MMSE filters.

6.2 Implementation Results

The implementation results for the LS channel estimator and MMSE filter are presented in Table 5 with different processing times. The estimators were implemented for 2×2 and 4×4 antenna systems, LTE pilot structure and for a 5 MHz bandwidth. The processing time of 71 μs corresponds to the case of delay in channel estimates and the shorter processing time corresponds to the no delay case shown in the bottom part of Fig. 8. The corresponding performance results were presented in Fig. 9. The detector latency was assumed to be half from the 71 μs OFDM symbol duration but the detector itself is not included in the complexity estimates. The LS estimator latency can then be 38 μs in the 2×2 antenna system and 33 μs in the 4×4 antenna system. The decoder latency [25] is also included in the latency calculations and each code word is assumed to be mapped to a single slot and

Table 5 Synthesis results for the LS and MMSE channel estimators with different latencies.

	No delay		Delay	
	LS	MMSE	LS	MMSE
	2×2			
Processing time	38 μs	38 μs	71 μs	71 μs
Clock frequency	95 MHz	95 MHz	51 MHz	51 MHz
Equivalent gates	3763	3213	3730	3213
Power consumption	8.3 mW	5.2 mW	4.8 mW	2.8 mW
	4×4			
Processing time	33 μs	33 μs	71 μs	71 μs
Clock frequency	146 MHz	146 MHz	102 MHz	68 MHz
Equivalent gates	3759	4549	3763	4375
Power consumption	13.2 mW	10.2 mW	8.9 mW	4.6 mW

not interleaved over multiple slots. As the LTE pilot structure contains pilot symbols for only two antennas in each slot even in the 4×4 antenna system, the complexity difference between the 2×2 and 4×4 results is not large. The gate count increases with the bandwidth in the LS estimator and the results can be scaled to higher bandwidths. The longer processing delay does not have a major impact on the complexity but the power consumption can be decreased.

The implementation results for the SAGE channel estimator are presented in Table 6. There are two target processing times for the SAGE estimator. The SAGE channel estimator has 31 μs in the no delay case to calculate the channel estimates in the 2×2 antenna system when the detector latency, the decoder latency of 5 μs, the symbol expectation latency of 1 μs and the IFFT [26] latency of 1 μs is subtracted from the OFDM symbol time. In the 4×4 antenna system, the decoder and IFFT have higher

Table 6 Synthesis results for the SAGE channel estimator with different latencies.

	Delay	No delay
	2×2	
Processing time	64 μs	31 μs
Symbols, S_i	1/2, 3	1/2, 4
Clock frequency	144 MHz	165 MHz
Equivalent gates	34.6 k	58.2 k
Power consumption	93 mW	189 mW
	4×4	
Processing time	59 μs	25 μs
Symbols, S_i	1/4, 4	1/4, 4
Clock frequency	104 MHz	147 MHz
Equivalent gates	113.4 k	210 k
Power consumption	257 mW	604 mW

Table 7 LS, MMSE and SAGE energy efficiency comparison.

Estimator	Pilots	Delay	Throughput	Energy/bit
LS	LTE	No	17.1 Mb/s	0.77 nJ/b
LS	LTE	Yes	11.6 Mb/s	0.767 nJ/b
MMSE	LTE	No	27.2 Mb/s	0.86 nJ/b
MMSE	LTE	Yes	19.6 Mb/s	0.388 nJ/b
SAGE	1 pilot	Yes	31.2 Mb/s	8.6 nJ/b

latencies and the processing time for SAGE channel estimation is only 25 μs. The longer processing times of 64 and 59 μs correspond to the case when channel estimation is performed during the detection of the following OFDM symbol.

The symbol expectation calculation was implemented with the architecture from [22] and the gate count of 5.5 k gates was added to the SAGE complexity in Table 6. The IFFT complexity was not considered in the total complexity. An IFFT block could be added to the receiver or the FFT with scaling could be reused, timing permitting. The LS estimator would be included in the receiver with SAGE channel estimator and the complexity and power estimates would have to be added together to get the total complexity of the SAGE channel estimator.

Implementation results for channel estimators have not been presented extensively in the literature. The approximate linear MMSE channel estimator from [13] uses the noise and correlation in calculating the coefficients. The implementation cost is 49 k gates but the algorithm is different from the MMSE in this paper, making a comparison difficult. Data carriers are exploited in channel estimation for calculating channel variations in [14]. The algorithm provides better performance in fast fading scenarios but the complexity of the channel estimator is 1901 k gates. Furthermore, the implementation was done for a wireless local area network (WLAN) system. An implementation of a decision feedback channel estimator for space-time block code system was introduced in [15]. However, the performance is not comparable to the spatial multiplexing system in this paper and the complexity for the one receive antenna implementation of [15] is higher than that of the SAGE estimator implementation for four antennas in this paper.

The LS estimator is used throughout the paper for obtaining the initial channel estimates from pilot symbols and the SAGE is used for updating the channel estimates. The use of DD LS estimation would be prohibitive because of the high complexity as stated in Section 5. With higher bandwidths or numbers of antennas, the time in which the SAGE channel estimation should be performed is shorter due to the increased decoder and FFT latencies. This results in higher complexity and power consumption. In terms of throughput per number of gates, the pilot only LS estimator uses the

least number of gates per bit. However, in higher velocities, the MMSE and SAGE estimators would greatly improve the performance. Furthermore, the throughput can be increased by decreasing the pilot symbol density and using the SAGE estimator in calculating the channel estimates.

The energy efficiency of the pilot based LS, MMSE and the DD SAGE channel estimators is presented in Table 7. The throughput is achieved in a 4×4 antenna system at 22 dB with 50 km/h user velocity as illustrated in Fig. 9. The throughput with perfect channel state information would be 32 Mb/s with pilot symbols in one OFDM symbol per slot. The power consumption of the LS estimator is included in all the estimators. The MMSE estimator with processing delay has the best energy efficiency but the SAGE estimator with delay can be used for improved throughput. When using the SAGE channel estimator at the receiver, less transmit power is needed for achieving the required throughput.

7 Conclusions

The performance of the DD SAGE channel estimation with the possibility of using it to improve the performance from the pilot symbol based estimators was considered. The least squares estimator was used in obtaining the channel estimates from pilot symbols. Time domain correlation of the channel estimates was exploited in the MMSE filter. The theoretical complexity of the SAGE algorithm and some complexity reducing modifications were presented. The implementation results for the pilot based LS estimator, the SAGE channel estimator and the MMSE filter were presented.

The complexity and power consumption of the LS and MMSE estimators are low. The delay after which the channel estimates from SAGE are available for detection has a high impact on the complexity and performance. The complexity and power consumption can be high when using the SAGE estimator with a short processing delay. A good performance-complexity trade-off can be achieved by allowing a longer processing delay for the SAGE estimator.

The MMSE filter and the SAGE estimator improve the pilot symbol based LS performance with high user velocities when the channel changes frequently between pilot symbols. The throughput can be increased by decreasing the pilot symbol density and transmitting data instead of pilot symbols. The SAGE estimator can then be used in calculating channel estimates when pilot symbols are not transmitted. The SAGE channel estimator would be a good choice for systems where training is performed in the beginning of the transmission or less frequently. The MMSE estimator is suitable for systems with high pilot densities.

Acknowledgments The authors would like to thank Calypto and Mentor Graphics for the possibility to use the Catapult C ® Synthesis tool.

References

1. 3rd Generation Partnership Project (3GPP); Technical Specification Group Radio Access Network. (2010). *Evolved universal terrestrial radio access E-UTRA; physical channels and modulation* (*release 10*) *TS 36.211* (*version 10.0.0*). Technical Report.
2. Cavers, J.K. (1991). An analysis of pilot symbol assisted modulation for Rayleigh fading channels. *IEEE Transactions on Vehicular Technology*, *40*(4), 686–693.
3. Kay, S.M. (1993). *Fundamentals of statistical signal processing: estimation theory*. Englewood Cliffs: Prentice-Hall.
4. Morelli, M., & Mengali, U. (2001). A comparison of pilot-aided channel estimation methods for OFDM systems. *IEEE Transactions on Signal Processing*, *49*(12), 3065–3073.
5. Barhumi, I., Leus, G., Moonen, M. (2003). Optimal training design for MIMO–OFDM systems in mobile wireless channels. *IEEE Transactions on Signal Processing*, *51*(6), 1615–1624.
6. Dempster, A.P., Laird, N.M., Rubin, D.B. (1977). Maximum likelihood from incomplete data via the EM algorithm. *Journal of the Royal Statistical Society*, *39*(1), 1–38.
7. Fessler, J., & Hero, A. (1994). Space-alternating generalized expectation-maximization algorithm. *IEEE Transactions on Signal Processing*, *42*(10), 2664–2677.
8. Xie, Y., & Georghiades, C.N. (2003). Two EM–type channel estimation algorithms for OFDM with transmitter diversity. *IEEE Transactions on Communications*, *51*(1), 106–115.
9. Panayirci, E., Şenol, H., Poor, H. (2010). Joint channel estimation, equalization, and data detection for OFDM systems in the presence of very high mobility. *IEEE Transactions on Signal Processing*, *58*(8), 4225–4238.
10. Ylioinas, J., & Juntti, M. (2009). Iterative joint detection, decoding, and channel estimation in turbo coded MIMO-OFDM. *IEEE Transactions on Vehicular Technology*, *58*(4), 1784–1796.
11. Li, Y., Cimini, L.J., Sollenberger, N.R. (1998). Robust channel estimation for OFDM systems with rapid dispersive fading channels. *IEEE Transactions on Communications*, *46*(7), 902–915.
12. Miao, H., & Juntti, M. (2005). Space-time channel estimation and performance analysis for wireless MIMO-OFDM systems with spatial correlation. *Transactions on Vehicular Technology*, *54*(6), 2003–2016.
13. Simko, M., Wu, D., Mehlfuehrer, C., Eilert, J., Liu, D. (2011). Implementation aspects of channel estimation for 3GPP LTE terminals. In *Proceedings of the European wireless conference, April 27–29*. Vienna.
14. Sun, M.-F., Juan, T.-Y., Lin, K.-S., Hsu, T.-Y. (2009). Adaptive frequency-domain channel estimator in 4×4 MIMO-OFDM modems. *IEEE Transactions on VLSI Systems*, *17*(11), 1616–1625.
15. Chen, H.-Y., Ku, M.-L., Jou, S.-J., Huang, C.-C. (2010). A robust channel estimator for high-mobility STBC-OFDM systems. *IEEE Transactions on Circuits Systems I*, *57*(4), 925–936.
16. Ketonen, J., Juntti, M., Ylioinas, J. (2010). Decision directed channel estimation for reducing pilot overhead in LTE-A. In *Proceedings of the annual asilomar conference on signals, systems, and computers. Nov. 7–10* (pp. 1503–1507). Pacific Grove: IEEE.

17. Ylioinas, J., Raghavendra, M.R., Juntti, M. (2009). Avoiding matrix inversion in DD SAGE channel estimation in MIMO-OFDM with M-QAM. In *Proceedings of the IEEE vehicular technology conference. Sept. 20–23* (pp. 1–5). Anchorage: IEEE.
18. 3rd Generation Partnership Project (3GPP); Technical Specification Group Radio Access Network. (2003). *Spatial channel model for multiple input multiple output (MIMO) simulations (3G TS 25.996 version 6.0.0 (release 6))*. 3rd Generation Partnership Project (3GPP), Tech. Rep.
19. Kunnari, E., & Iinatti, J. (2007). Stochastic modelling of Rice fading channels with temporal, spatial and spectral correlation. *IET Communications*, *1*(2), 215–224.
20. Wong, K., Tsui, C., Cheng, R.K., Mow, W. (2002). A VLSI architecture of a K-best lattice decoding algorithm for MIMO channels. In *Proceedings of the IEEE international symposium on circuits and systems. May 26–29* (Vol. 3, pp. 273–276). Scottsdale: IEEE.
21. Lee, J., Lou, H.-L., Toumpakaris, D., Cioffi, J. (2006). SNR analysis of OFDM systems in the presence of carrier frequency offset for fading channels. *IEEE Transactions on Wireless Communications*, *5*(12), 3360–3364.
22. Ketonen, J., Juntti, M., Cavallaro, J. (2010). Performance-complexity comparison of receivers for a LTE MIMO-OFDM system. *IEEE Transactions on Signal Processing*, *58*(6), 3360–3372.
23. Martin, G., & Smith, G. (2009). High-level synthesis: past, present, and future. *IEEE Design Test of Computers*, *26*(4), 18–25.
24. Calypto. (2013). *Catapult overview*. Tech. Rep. http://calypto.com/en/products/catapult/overview.
25. Sun, Y., Zhu, Y., Goel, M., Cavallaro, J. (2008). Configurable and scalable high throughput turbo decoder architecture for multiple 4G wireless standards. In *Proceedings of the IEEE international conference on application-specific systems, architectures and processors (ASAP). July 2–4* (pp. 209–214). Leuven: IEEE.
26. Babionitakis, K., Manolopoulos, K., Nakos, K., Chouliaras, V. (2006). A high performance VLSI FFT architecture. In *Proceedings of the IEEE international conference on electronics, circuits and systems December 10–13* (pp. 810–813). Nice: IEEE.

Johanna Ketonen received her M.Sc. (Tech.) degree in Electrical and Information Engineering and Dr.Sc. (Tech.) degree in Communications Engineering from the University of Oulu, Oulu, Finland in 2007 and 2012, respectively. She is currently working as a postdoctoral researcher at the Department of Communications Engineering, University of Oulu, Finland. Her main research interests are in the implementation oriented study of receiver algorithms for mobile systems.

Markku Juntti received his M.Sc. (Tech.) and Dr.Sc. (Tech.) degrees in Electrical Engineering from University of Oulu, Oulu, Finland in 1993 and 1997, respectively. Dr. Juntti was with University of Oulu in 1992–98. In academic year 1994–95 he was a Visiting Scholar at Rice University, Houston, Texas. In 1999–2000 he was a Senior Specialist with Nokia Networks. Dr. Juntti has been a professor of communications engineering at University of Oulu, Department of Communication Engineering and Centre for Wireless Communications (CWC) since 2000. His research interests include signal processing for wireless networks as well as communication and information theory. He is an author or co-author in some 200 papers published in international journals and conference records as well as in book *WCDMA for UMTS* published by Wiley. Dr. Juntti is also an Adjunct Professor at Department of Electrical and Computer Engineering, Rice University, Houston, Texas, USA.

Jari Ylioinas received his M.Sc. (Tech.) and Dr.Sc. (Tech.) degrees in Electrical Engineering from University of Oulu, Oulu, Finland in 2004 and 2010, respectively. During 2003-2010 he was with Centre for Wireless Communications (CWC) at the University of Oulu, working as a research scientist and project manager. In 2010, he joined Nokia Siemens Networks and is currently working as a research specialist and a project manager. His main research interests are in physical layer as well as MAC layer algorithms in HSPA and LTE-A systems.

Joseph R. Cavallaro received the B.S. degree from the University of Pennsylvania, Philadelphia, Pa, in 1981, the M.S. degree from Princeton University, Princeton, NJ, in 1982, and the Ph.D. degree from Cornell University, Ithaca, NY, in 1988, all in electrical engineering. From 1981 to 1983, he was with AT&T Bell Laboratories, Holmdel, NJ. In 1988, he joined the faculty of Rice University, Houston, TX, where he is currently a Professor of electrical and computer engineering. His research interests include computer arithmetic, VLSI design and microlithography, and DSP and VLSI architectures for applications in wireless communications. During the 1996-1997 academic year, he served at the National Science Foundation as Director of the Prototyping Tools and Methodology Program. He was a Nokia Foundation Fellow and a Visiting Professor at the University of Oulu, Finland in 2005 and continues his affiliation there as an Adjunct Professor. He is currently the Associate Director of the Center for Multimedia Communication at Rice University.